Journal of Solid State Chemistry **143,** 1–8 (1999)
Article ID jssc.1998.8046, available online at http://www.idealibrary.com on IDEAL®

Electronic Structure of the Organic Conductors κ-$ET_2Cu(SCN)_2$ and κ-$ET_2Cu[N(CN)_2]Br$ Studied Using Soft X-ray Absorption and Soft X-ray Emission

Cristian B. Stagarescu,[1] Laurent-C. Duda, and Kevin E. Smith[2]

Department of Physics, Boston University, Boston, Massachusetts, 02215

D.-K. Seo and M.-H. Whangbo

Department of Chemistry, North Carolina State University, Raleigh, North Carolina 27695-8204

Denis Jeromé

Laboratoire de Physique des Solides, Université de Paris-Sud, 91405 Orsay, France

Robert C. Haddon

Department of Chemistry, University of Kentucky, Lexington, Kentucky 40506-0055

James S. Brooks

Department of Physics, Florida State University, Tallahassee, Florida 32306-4000

and

Jinghua Guo and Joseph Nordgren

Department of Physics, Uppsala University, Box 530, 75121 Uppsala, Sweden

Received June 24, 1998; in revised form September 28, 1998; accepted September 29, 1998

The problem of resolving molecular components of the electronic structure of complex, organic solids with respect to their chemical and orbital character has been approached using core-level photon spectroscopies. Specifically, the bulk C 2*p* occupied and unoccupied partial densities of states (PDOS) of the organic superconductors κ-$ET_2Cu(SCN)_2$ and κ-$ET_2Cu[N(CN)_2]Br$ were measured using a combination of high-resolution soft X-ray absorption (SXA) and soft X-ray emission (SXE). The PDOS was also calculated using a tight binding model, and the measured spectra compared directly to that predicted by the calculations. The emission and absorption spectra from both materials were found to be quite similar, reflecting mostly contributions from the common conductive ET layers. The presence of two nonequivalent carbon sites of the ET molecule was identified in the SXA spectra. Contributions from the π and σ states were identified in the emission spectra. The occupied C 2*p* bandwidth was found to be approximately 17 eV. An observed dependence of the SXE spectra on the excitation energy is partly accounted for by a simple model that considers the presence of the two nonequivalent ET carbon sites. We also find evidence in the SXE spectra for a high degree of localization in the lowest unoccupied states.

I. INTRODUCTION

The charge transfer salts κ-$ET_2Cu[N(CN)_2]Br$ and κ-$ET_2Cu(SCN)_2$ are organic superconductors with transition temperatures of 10.4 and 11.6 K, respectively (1, 2). They belong to the κ-phase structural family of the type κ-ET_2X, where ET stands for the organic donor molecule of bis(ethylenedithio)-tetrathiafulvalene (BEDT-TTF) and X for inorganic acceptor radical. Their crystal structure consists of a stacking of two alternating layers: a nonconducting inorganic layer in which the acceptor radicals ($Cu(SCN)_2$ or $Cu[N(CN)_2]Br$) build a zigzag planar network, and a conducting organic layer containing ET dimers.

[1] On leave from the Institute of Microtechnology, Bucharest, Romania.
[2] To whom correspondence should be addressed. E-mail address: ksmith@bu.edu.

0022-4596/99 $30.00

The overlap of the ET-derived π- molecular orbitals provides a two-dimensional conductive network in the organic layers in the form of narrow quasi-planar bands, leading to a strong anisotropy in the electrical conductivities parallel and perpendicular to the layers.

Most of the information concerning the electronic structure of these materials has come from transport and magnetic resonance measurements, which are limited to probing the structure close to the Fermi surface. A more comprehensive measurement of electronic structure in these molecular conductors over a large range of energies is clearly needed. Photoemission spectroscopy is a ubiquitous probe of the occupied electronic states in solids (3–5) and has been applied to various organic conductors (6–11). Nevertheless, spectroscopic probes that make it possible to resolve directly contributions to the bulk electronic structure with respect to their atomic and orbital character are highly relevant for organic solids since they help to discern signatures of the molecular components. We report here a study of the bulk electronic structure in κ-$ET_2Cu(SCN)_2$ and κ-$ET_2Cu[N(CN)_2]Br$ using synchrotron radiation excited high-resolution soft X-ray emission (SXE) and soft X-ray absorption (SXA). In particular, we have used SXE and SXA to measure the full C 2*p* contribution to the occupied and unoccupied electronic structure in both materials. The absorption or emission of a soft X-ray photon involves participation of localized atomic core levels, and the predominance of intra-atomic processes leads to chemical and atomic-site sensitivity. Furthermore, dipole-selection rules restrict the orbital character of the probed occupied or unoccupied states. Thus in the simplest interpretation, SXE and SXA spectra represent the bulk site-projected and orbital symmetry restricted partial density of occupied and unoccupied states, respectively. We compare our measurement of the C 2*p* partial density of states to the results of an extended Hückel tight binding calculation of the C 2*p* states.

II. EXPERIMENTAL DETAILS

The experiments were carried out at beamline 7 of the advanced light source (12). The beamline is equipped with a 5-cm-period undulator and a spherical grating monochromator and delivers a high flux of soft X-rays in the energy range from 60 to 1000 eV at a typical resolving power of 2000. The SXA spectra were taken in the sample drain current mode, with an energy resolution of 0.250 eV at energies corresponding to the C 1*s* absorption edge (approximately 290 eV); the photon beam was incident at 45° to the sample normal. The SXE spectra were recorded with a Nordgren-type grazing-incidence grating spectrometer (13). For SXE measurements, the beamline monochromator resolution was set to 0.250 eV and the spectrometer resolution set to 0.50 eV. A typical SXE spectrum with reasonable signal to noise ratio was recorded in 1 h at this resolution. The samples used were single crystals having typical dimensions of $2 \times 2 \times 0.5$ mm, mounted with a vacuum compatible conductive epoxy on a Ta sample holder. The base pressure of the spectrometer chamber was 1×10^{-8} Torr, which is sufficient for these bulk probes, and surface effects were not being studied.

III. RESULTS AND DISCUSSION

III.1. Soft X-Ray Emission: Occupied States of C-2p Character

In Fig. 1 we present X-ray emission spectra from κ-$ET_2Cu[N(CN)_2]Br$ and κ-$ET_2Cu(SCN)_2$. The SXE spectra of both materials have been taken under identical conditions, with an excitation energy of 289.6 eV. This value matches the energy position of a prominent empty spectral feature having a highly similar energy position and shape in the SXA spectra of the two compounds (see Section III.2). The intense sharp feature centered at 289.6 eV (scaled down in Fig. 1) is the elastic peak, resulting from the direct recombination of the excited electron, and presumably also

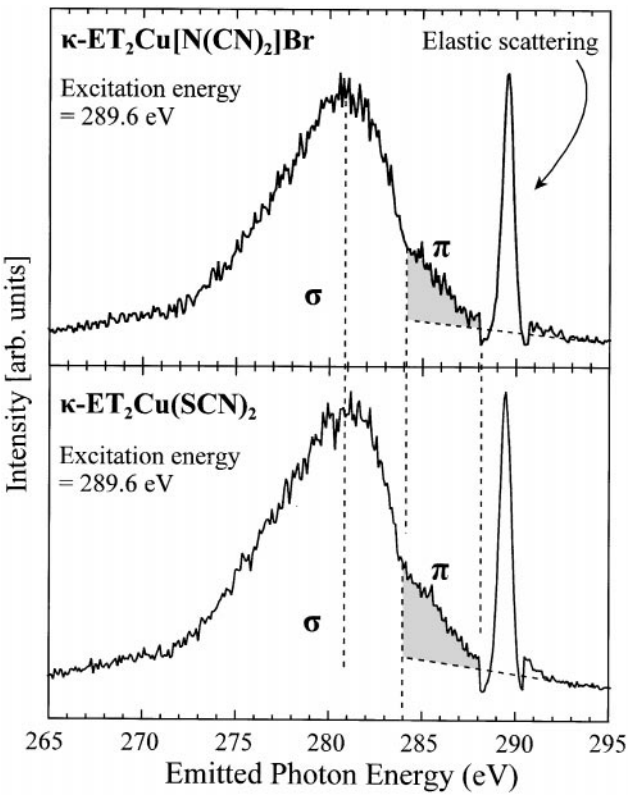

FIG. 1. Comparison of the C-1*s* SXE spectra of κ-$ET_2Cu(SCN)_2$ and κ-$ET_2Cu[N(CN)_2]Br$, with $h\nu_{exc.} = 289.6$ eV. The intensities of the very strong elastic peaks have been scaled down to allow the valence band emission to be resolved. Note the high degree of similarity between emissions from the two materials.

from some diffuse scattering of the incoming light. This peak appears at an energy equal to the excitation energy and was used to set the energy scale of the SXE spectra (see Section III.3). The photons emitted at energies below the elastic peak result generically from C $2p \rightarrow 1s$ emission) events. Since the final state in X-ray emission contains a hole in the valence band, one expects that soft X-ray emission spectra reflect the ground state density of states (DOS) if the final state rule is valid (14). The final state rule states that the spectral features that appear in X-ray spectroscopy correspond to the theoretical partial DOS (PDOS) calculated with the final state potential. The overall width of the occupied C $2p$ PDOS is found from Fig. 1 to be approximately 17.0 eV for both conductors. As expected for molecular crystals formed from organic molecules, the π-bands fill the region of binding energies from the Fermi level (E_F) down to approximately 4.5 eV, while the σ-bands form the broad, dominant feature centered at approximately 7.5 eV binding energy (15). The SXE spectra from κ-$ET_2Cu(SCN)_2$ and κ-$ET_2Cu[N(CN)_2]Br$ are highly similar. This indicates that the C $2p$ emission originates primarily from the common ET conductive layers of the two materials and that we cannot discern the small, possibly different, contribution to the C $2p$ PDOS from of the carbon atoms residing in the inorganic layers.

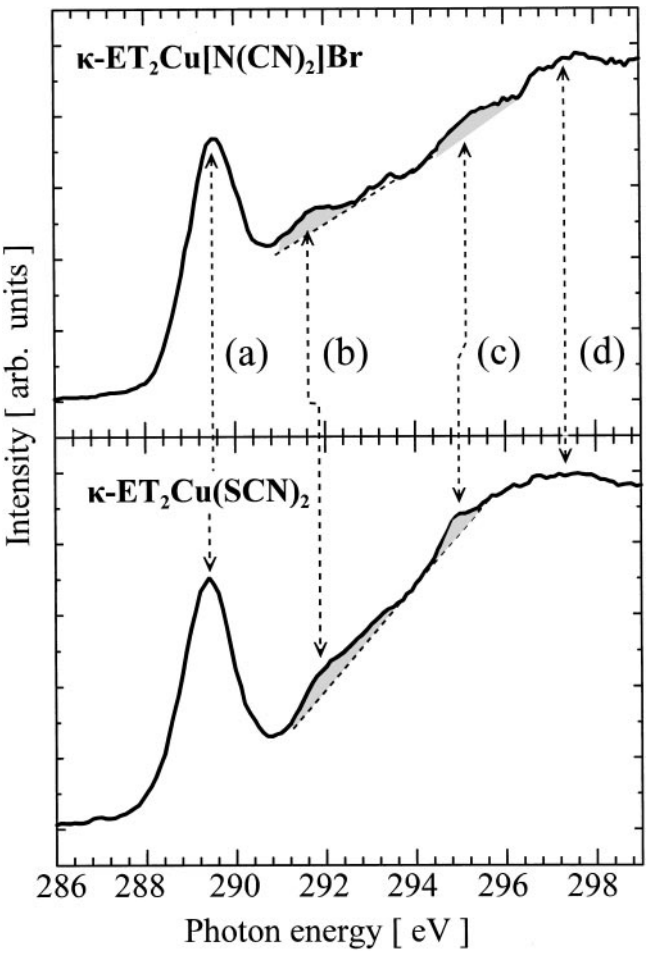

FIG. 2. SXA spectra for κ-$ET_2Cu(SCN)_2$ (bottom) and κ-$ET_2Cu[N(CN)_2]Br$ (top). See text for details.

III.2. Soft X-ray Absorption: Unoccupied States of C 2p Character

Before describing our SXA data some clarification regarding the use of the LUMO/HOMO (lowest unoccupied/highest occupied molecular orbitals) terms is required. In the formal, theoretical sense LUMO (HOMO) is identified with that single, unoccupied (occupied) molecular orbital having the lowest (highest) energy in a calculated molecular orbitals energy scheme (16). The spectral features corresponding to the lowest unoccupied state in SXA, and highest occupied state in SXE cannot be interpreted directly as the LUMO, and respectively HOMO, in the strict, theoretical sense, for two reasons. First, with the resolution available in our study SXA and SXE cannot resolve each of the many closely spaced molecular orbitals defining the HOMO–LUMO gap of a calculated molecular orbitals scheme (16). Second, it is known that spectral features of a molecular solid are similar but broadened in comparison to the gas-phase spectrum of the comprising molecular species (9–11, 15). Figure 2 presents SXA spectra from κ-$ET_2Cu(SCN)_2$ and κ-$ET_2Cu[N(CN)_2]Br$. Clearly, these spectra are quite similar: above the C $1s$ absorption edge (approximately 288.0 eV) four spectral features (a, b, c, d) are common to both spectra. By comparing to the general characteristics of the NEXAFS spectra of large organic compounds (17), features (a) and (d) are identified with the π* (ET-(C=C) $1s$) resonance and the σ* resonance of the ET molecule. Peak (a) at a photon energy of 289.6 eV in κ-$ET_2Cu(SCN)_2$ results from the excitation of electrons from the C $1s$ core level of the double bonded ET carbon atoms into the previously empty states derived from the lowest unoccupied molecular orbitals of ET (designated LUMO-ET). An assignment for the spectral features (b) and (c) can be made by referring to a previous X-ray photoemission spectroscopy (XPS) study. We believe the validity of this reference to XPS results (a partially surface sensitive technique) to be strengthened by recent STM studies (18–20) in which the surface of κ-$ET_2Cu(SCN)_2$ appears to be molecularly flat, having a structure in agreement with the bulk structure determined by X-ray diffraction. In their XPS work Itti *et al.* (21) found three well separated features in the C $1s$ XPS spectrum of κ-$ET_2Cu(SCN)_2$, at binding energies of approximately 285.5, 287.5, and 291.0 eV. By relating the relative intensities of the XPS peaks to the number of nonequivalent carbon sites, the lowest binding energy peak

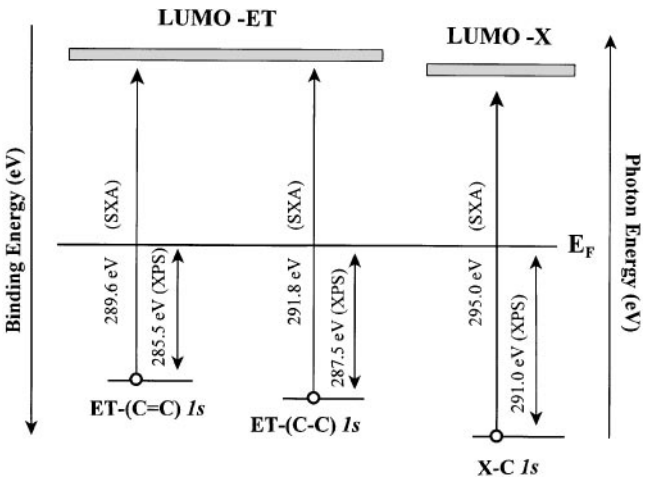

FIG. 3. Schematic energy diagram for the C 1*s* core levels and LUMO-s of κ-$ET_2Cu(SCN)_2$. LUMO-ET represents states derived from the lowest unoccupied molecular orbital for the ET molecule, LUMO-X is the equivalent for $Cu(SCN)_2$ (= X).

(285.5 eV) was associated to the six double bonded (C=C) carbon atoms of ET, the peak at a binding energy of 287.5 eV to the four single bonded (C–C) atoms of ET and a weak feature at a binding energy of 291.0 eV to the two equivalent carbon atoms of the $Cu(SCN)_2$ anion. This situation is illustrated in Fig. 3. The difference in photon energy between features (a) and (b) in Fig. 2 (approximately 2.6 eV for κ-$ET_2Cu(SCN)_2$) is similar to the 2-eV difference between the binding energies of the ET–(C=C) 1*s* and ET–(C–C) 1*s*. Therefore we associate (b) to absorption from the ET–(C–C) 1*s* core levels into LUMO-ET. Likewise, the weak SXA feature (c) appearing on the leading edge of the σ resonance at approximately 5.4 eV above feature (a) is tentatively associated to transitions from the "inorganic" C 1*s* into the LUMO of the inorganic radicals (designated LUMO-X). Since the XPS binding energies and the SXA photon energies have not been measured on the same experimental setup, the absolute energy position of the LUMO-s above E_F is not exact. Note that the (a)/(b) intensity ratio in the SXA spectra departs considerably from what one would expect on a simple argument based on counting the number of nonequivalent chemical sites, i.e., 6/4. However, a much smaller intensity of the absorption from the ET–(C–C) 1*s* into the LUMO-ET is consistent with theoretical studies that have found that the LUMO-ET is essentially a π-type molecular orbital and hence has little contribution from the atomic orbitals of the singly bonded carbon atoms (22, 23). The data thus confirm that most of the charge density of the LUMO-ET is located over the central part of the ET molecule, containing a double bonded carbon atom, with very little weight present over the outer, single bonded carbon atoms.

III.3. Comparison of Measured and Calculated C2p PDOS of κ-$ET_2Cu[N(CN)_2]Br$

In order to understand the SXE spectra more fully, we have performed a detailed calculation of the occupied and unoccupied electronic structure for κ-$ET_2Cu[N(CN)_2]Br$ using the extended Hückel tight binding (EHTB) method (24) and the C 2*p* PDOS plots were calculated based on the atomic population analysis (25). The atomic parameters needed for these calculations were taken from the previous studies (26).

Since results from two different measuring techniques will be compared to the calculated PDOS, the procedure used for setting a common binding energy scale must be discussed. First, the π*(ET–(C=C)) SXA resonance was aligned over the elastic peak, since as indicated, the SXE spectrum was taken with 289.6 eV excitation energy. This places both the SXA and SXE spectra on a common photon energy scale. Next, the high photon energy limit of the SXE spectrum was aligned to the Fermi level of the calculated PDOS. In the absence of an XPS binding energy measurement done in conjunction with the SXA/SXE measurements, this assignment of E_F in the experimental spectra and its alignment with the calculated PDOS remains an arbitrary parameter. The SXE and SXA spectra are compared to the calculation in Fig. 4. The measured spectra are presented in the top panel, and the calculation in the bottom panel. The calculated C 2*p* PDOS is presented for C atoms in both the ET_2 layers and in the "X", $Cu[N(CN)_2]Br$ layers, together with the total C 2*p* PDOS. The calculated PDOS plots are smoothed via a Gaussian function with $\delta = 0.5$ (25).

We find good overall agreement of the experimental and calculated *occupied* PDOS. The center of the dominant, broad σ-feature in the SXE spectrum coincides with the most intense feature in the σ-part of the calculated PDOS curve. In addition, the high binding energy limit of the calculated PDOS (as indicated by the small spectral feature situated at approximately 17.0 eV binding energy) corresponds well to the low-photon energy cutoff of the SXE spectrum. As for the *unoccupied* states, the comparison between the SXA spectrum and the calculation is not as straightforward. The three features (a, b, c) of the SXA spectrum can be assigned experimentally following the discussion in Section III.2. However, there is clearly little obvious correspondence between the energy positions of the LUMO-ET and LUMO-X features of the calculated unoccupied C 2*p* PDOS and the spectral features of the SXA spectrum. It should be noted that *relative* energies of the ET molecules and the X anions calculated using the EHTB method are not expected to be reliable due to neglect of the effect of charge transfer from ET to X on the atomic orbital parameters. In general, the energy levels of a molecular species are raised when it gains electron density and are lowered when it loses electron density (27). Consequently,

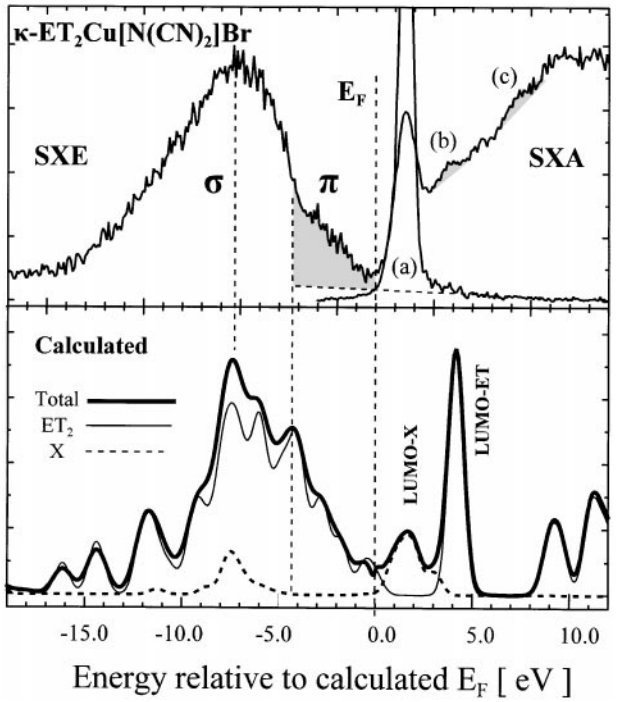

FIG. 4. Comparison of the measured C 2*p* occupied (SXE) and unoccupied (SXA) PDOS of κ-$ET_2Cu[N(CN)_2]Br$ with the calculated PDOS. The ET and $Cu[N(CN)_2]Br$ resolved PDOS curves are shown as calculated. The total C 2*p* calculated PDOS is broadened with a convolution function simulating the effect of core-hole lifetime (Lorentzian) and instrumental resolutions (Gaussian). The spectra are plotted against the energy scale of the calculated PDOS. See text for details.

from the viewpoint of the calculated PDOS plots presented in Fig. 4, a more correct relative ordering of the energy levels of the ET and X units would be obtained by raising the energy levels of the X and by lowering those of the ET. A further important consideration is that SXA records the energy position of unoccupied states with respect to core levels, which lie at various binding energies in the case of nonequivalent atomic sites (see Fig. 3). Therefore appropriate differences in binding energy should be taken into account for the energy positions of absorption features (a), (b), and (c) in Fig. 4 before making a comparison with the calculated PDOS curve. XPS core level binding energy data for κ-$ET_2Cu[N(CN)_2]Br$ is not available, but using the C 1*s* data from κ-$ET_2Cu(SCN)_2$ we can make the following argument. There is a difference in C 1*s* binding energy of 5.5 eV between the double bonded carbon in ET–(C=C) and the carbon in the inorganic layer, X. Subtracting this 5.5 eV from the photon energy of SXA feature (c), we obtain a value of approximately 2.0 eV for the this feature *relative to* E_F. This is close to the energy position above E_F of the calculated LUMO for the X layer. Thus we associate feature (c) with LUMO-X. Considering features (a) and (b), both were assigned in Section III.2 to transitions to the LUMO-ET. Finally, we note that the effect of the localized C 1*s* core hole on π^* states has been studied for both crystalline (graphite) (17) and molecular (C_{60}) (28) extended π-electron systems. The interaction between the excited π^* electron and the C 1*s* core hole, manifested mainly as a screening distortion of the local potential, was found to induce a downward energy shift of the π^* resonances and must be taken into account for a proper description of the SXA spectra. In the case of our ET-based molecular crystals the presence of a similar screening effect is at least partially responsible for the misalignment between the calculated LUMO-ET and the strong π^*(ET–(C=C)) SXA resonance.

III.4. Excitation Energy Dependence of SXE Spectra

We have observed a strong dependence of the C 2*p* SXE spectra on the energy of the photon used to create the C 1*s* core hole for both κ-$ET_2Cu(SCN)_2$ and κ-$ET_2Cu[N(CN)_2]Br$. Figure 5 shows SXE spectra from κ-$ET_2Cu[N(CN)_2]Br$ recorded for two *excitation* energies: $h\nu_{exc.} = 289.6$ eV, which corresponds to excitations into the π^*(ET–(C=C)) state, and $h\nu_{exc.} = 298.0$ eV, corresponding to transitions into the σ^* state (see Fig. 1). As the excitation photon energy increases, the emission from the π-occupied bands becomes more intense, and a shift of the dominant part of the SXE spectrum to higher *emitted* photon energies is observed. At the same time emission from the bottom of the C 2*p* band remains at a constant photon energy. A similar effect is observed in emission from κ-$ET_2Cu(SCN)_2$ and is presented in Fig. 6.

We can distinguish two regimes in Fig. 6. For excitation energies at and above 291.8 eV (aside from the expected reduction of the intensity of the elastic peak with the increase of the excitation energy) the SXE spectra are largely independent of excitation energy, showing a strong spectral weight in the π region. However, as the excitation energy is lowered through the prominent π^*(ET–(C=C)) resonance (289.6 eV) toward the absorption edge, a continuous shift of the emission spectrum to lower photon energies and a reduction of the π-spectral weight is observed.

The appearance of this shift can be understood in a simplified fashion as illustrated in Fig. 7. Figure 7a corresponds to the situation where the excitation energy is set at 289.6 eV, i.e., sufficient to excite electrons from the double bonded ET–(C=C) 1*s* core levels into the LUMO on the ET molecule, but not sufficient to excite the more tightly bound single bonded ET-(C-C) 1*s* electrons. Figure 7b corresponds to the situation where the excitation energy is increased just enough to allow the excitation of ET–(C–C) 1*s* into LUMO-ET. In this configuration, the ET–(C=C) 1*s* electrons will now be excited into states situated approximately 2 eV above the LUMO-ET. Consequently, the measured SXE spectrum will now contain two partially overlapping

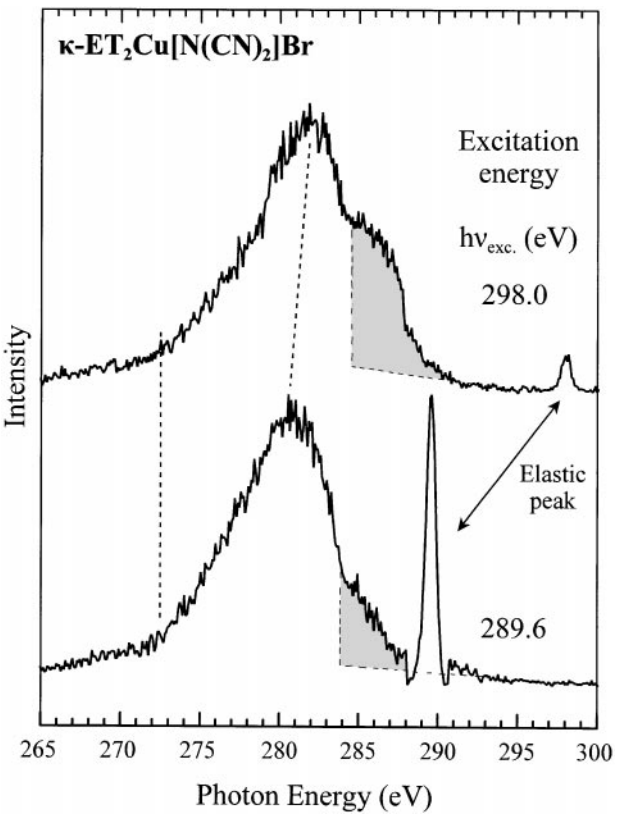

FIG. 5. Spectral changes in the C 2*p* SXE from κ-$ET_2Cu[N(CN)_2]Br$ with excitation energy. Excitation energies are indicated; dashed lines are guides for the eye. The shaded region corresponds to emission from π states.

components, one of which appears at a higher *photon* energy and thus appears to lie at smaller *binding* energy. This simple model accounts for much of the spectral behavior shown in Figs. 5 and 6. For example, as illustrated in Fig. 7, in both cases the low photon energy cutoff of the SXE spectra should be at the same energy, since this is determined by transitions from the bottom of the occupied C 2*p* bands into the ET–(C=C) 1*s* core hole. This is indeed what is observed in Figs. 5 and 6: emission from the bottom of the valence band appears at a constant photon energy and is independent of the excitation energy, above threshold. The apparent increase in π emission and band width with increasing excitation photon energy can be explained as being due to the fact that there are now two SXE channels open. The partial overlap of emission due to transitions into (C=C) and (C–C) states leads to partial overlap of the two corresponding spectra, and so to an enhancement of emission near the top of the band, i.e. in the π region, and to an increase in the measured band width (in photon energy).

Note, however, that for the lower three spectra of Fig. 6 there is a shift of the emission maximum to higher photon energies as the excitation energy is tuned through the low energy side of the π^*(ET–(C=C)) resonance (see Fig. 2). Only the ET–(C=C) $1s \rightarrow$ LUMO excitation channel is open here, and thus this shift cannot be an artifact due to overlap of emission into the (C–C) states. Similar behavior near excitation threshold has been observed for a variety of molecular and solid-state systems (29, 30) and has been interpreted as a screening effect (31). In this model, as the excitation energy is resonantly tuned across an empty state with a localized character, the screening of the core hole by the excited electron causes energy shifts and possibly intensity variations of the SXE spectra. Our observation of an energy shift in the emission spectra at threshold excitation thus probably indicates that the unoccupied states constructed from the ET-LUMO are partially localized; i.e., even when the ET molecules form a κ-ET_2X organic solid, the relatively small overlap of their molecular orbitals preserves their molecular identity. Finally, it should be pointed out that the preceding arguments have been based exclusively on the electronic structure of the ET molecule only. The role of the C atoms in the inorganic layers is likely to be quite small, and preliminary experiments find shifts and intensity

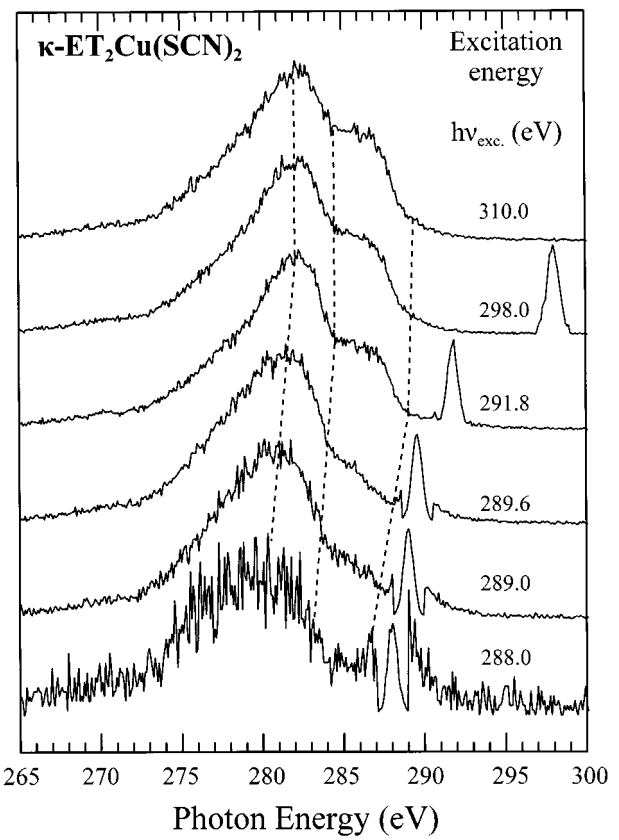

FIG. 6. Spectral changes in the C 2*p* SXE from κ-$ET_2Cu(SCN)_2$ with excitation energy. Excitation energies are indicated adjacent to each spectra. Lines are guides to the eye.

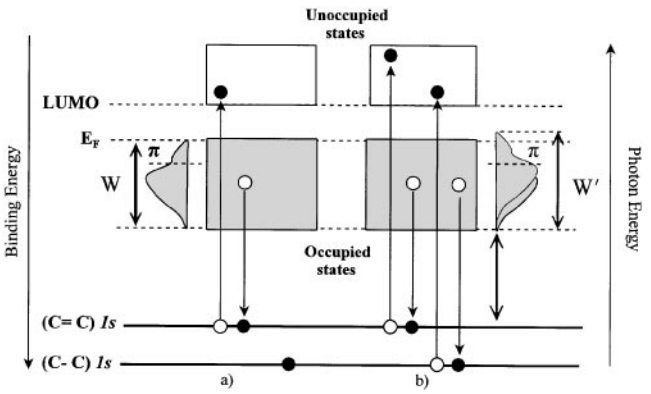

FIG. 7. Schematic representation of the SXA and SXE processes in the presence of two nonequivalent core levels. See text for details.

changes similar to those in Fig. 6 for the C 2*p* SXE spectra of β-ET_2IBr_2, an ET-based compound that contains no carbon atoms in its inorganic layers (32).

IV. SUMMARY

Using a combination of high-resolution SXA and SXE, we have measured for the first time the C 2*p* contributions to the occupied and unoccupied states in the organic superconductors κ-$ET_2Cu(SCN)_2$ and κ-$ET_2Cu[N(CN)_2]Br$. The signature of two nonequivalent carbon sites of the ET molecule was identified in the absorption spectra, and the relative intensity of their corresponding absorption features agrees well with the calculated asymmetry of the spatial distribution of the LUMO-ET. The occupied C 2*p* PDOS from the ET layers consists of two well-defined parts: a low-binding energy region of π-states (from E_F to approximately 4.5 eV binding energy) and a region of higher spectral weight (centered at approximately 7.5 eV) dominated by σ-states. This is consistent with our calculations and the general characteristics of molecular organic crystals. The overall bandwidth of the C 2*p* states was found to be approximately 17.0 eV. The observed dependence of the SXE spectra with the excitation energy is partly accounted for by a simple model in which either one or both of the allowed X-ray emission channels corresponding to the two nonequivalent ET-C 1*s* core levels are open depending on the value of the excitation energy. Where the emission is allowed to occur only into the double bonded ET–(C=C) carbon atoms, a continuous shift of the SXE spectra with the excitation energy is observed. We interpret this as a manifestation of the screening of ET–(C=C) 1*s* core hole by the electrons excited into the ET-LUMO and therefore as an indication of the degree of localization preserved in the molecular solids by the LUMO-ET states.

ACKNOWLEDGMENTS

This work was supported in part by the National Science Foundation under DMR-9501174. The NCSU research was supported by the Department of Energy under DE-FG05-86ER45259. The ALS is operated by the University of California as part of the U.S. Department of Energy, Office of Basic Energy Sciences. L.-C.D. gratefully acknowledges the Swedish Natural Research Council for a postdoctoral fellowship at Boston University. Charles Agosta is acknowledged for providing a β-ET_2IBr_2 sample.

REFERENCES

1. A. M. Kini, U. Geiser, H. H. Wang, K. D. Carlson, and J. D. Williams, *Inorg. Chem.* **29,** 2555 (1990).
2. H. Urayama, H. Yamochi, G. Saito, S. Sato, A. Kawamoto, J. Tanaka, T. Mori, Y. Maruyama, and H. Inokuchi, *Chem. Lett*. **1988,** 55 (1988).
3. M. Cardona and L. Ley (Eds.), "Photoemission in Solids," Springer Verlag, Berlin, 1978.
4. S. D. Kevan (Ed.), "Angle Resolved Photoemission," Elsevier, Amsterdam, 1991.
5. K. E. Smith and S. D. Kevan, *Prog. Solid State Chem.* **21,** 49 (1991).
6. R. Liu, H. Ding, J. C. Campuzano, H. H. Wang, J. M. Williams, and K. D. Carlson, *Phys. Rev.* B **51**(19), 13000 (1995).
7. R. Liu, H. Ding, J. C. Campuzano, H. H. Wang, J. M. Williams, and K. D. Carlson, *Phys. Rev.* B, **51,**(9), 6155 (1995).
8. M. Yoshimura, H. Shigekawa, T. Mori, M. Kageshima, H. Kato, Y. Sakisaka, G. Saito, and A. Kawazu, *Jpn. J. Appl. Phys.* **31,** 1341 (1992).
9. S. Söderholm, B. Loppinet, and D. Schweitzer, *Synth. Met.* **62,** 187 (1994).
10. S. Söderholm, P. R. Varekamp, and D. Schweitzer, *Phys. Rev.* B **52**(13), 9629 (1995).
11. S. Söderholm, R. T. Girard, and D. Schweitzer, *Phys. Rev.* B **55**(7), 4267 (1995).
12. T. Warwick, P. Heinemann, D. Mossessain, W. Mackinney, and H. Padmore, *Rev. Sci. Inst*. **66,** 2037 (1995).
13. J. Nordgren, G. Bray, S. Cramm, R. Nyholm, J.-E. Rubensson, and N. Wassdahl, *Rev. Sci. Inst*. **60,** 1690 (1989).
14. U. von Barth and G. Grossmann, *Phys. Rev.* B **25,** 5150 (1982).
15. W. D. Grobman and E. E. Koch, *in* "Photoemission in Solids" (L. Ley and M. Cardona, Eds.), Springer-Verlag, Berlin, 1979.
16. J. Shumway, S. Chattopadhyay, and S. Satpathy, *Phys. Rev.* B **53**(10), 6677 (1996).
17. J. Stöhr, "NEXAFS Spectroscopy." Springer, Berlin, 1992.
18. S. Yoon, W. F. Smith, M. Yoo, and A. L. deLozanne, *Phys. Rev.* B **47**(8), 4802 (1993).
19. M. Yoshimura, H. Shigekawa, H. Nejoh, G. Saito, Y. Saito, and A. Kawazu, *Phys. Rev.* B **43**(16), 13590 (1991).
20. R. Fainchtein, S. T. D'Arcangelis, S. S. Yang, and D. O. Cowan, *Science* **256,** 1012 (1992).
21. R. Itti, H. Mori, K. Ikeda, I. Hirabayashi, N. Koshizuka, and S. Tanaka, *Physica C* **185–189,** 2673 (1991).
22. M.-H. Whangbo, J. M. Williams, P. C. W. Leung, M. A. Beno, T. J. Emge, and H. H. Wang, *Inorg. Chem.* **24,** 3500 (1985).
23. E. Demilrap and W. A. Goddard, *J. Phys. Chem.* **98,** 9781 (1994).
24. M.-H. Whangbo and R. Hoffmann, *J. Am. Chem. Soc*. **100,** 6093 (1978).
25. E. Canadell and M.-H. Whangbo, *Chem. Rev.* **91,** 965 (1991).
26. M.-H. Whangbo, J. J. Novoa, D. Jung, J. M. Williams, A. M. Kini, H. H. Wang, U. Geiser, M. A. Beno, and K. D. Carlson, *in* "Organic Superconductivity" (V. Z. Kresin and W. A. Little, Eds.). Plenum, New York, 1990.
27. T. A. Albright, J. K. Burdett, and M.-H. Whangbo, "Orbital Interactions in Chemistry." Wiley, New York, 1985.

28. B. Wästberg, S. Lunell, C. Enkvist, P. A. Brühwiler, A. J. Maxwell, and N. Mårtensson, *Phys. Rev.* B **50**(17), 13031 (1994).
29. P. Skytt, P. Glans, K. Gunnelin, J. Guo, and J. Nordgren, *Phys. Rev.* A **55**(1), 134 (1996).
30. W. L. O'Brien, J. Jia, Q.-Y. Dong, and T. A. Callcott, *Phys. Rev. Lett.* **70**(2), 238 (1993).
31. H. Ågren, Y. Luo, F. Gelmukhanov, H. Jørgen, and A. Jensen, *J. Electron Spectrosc. Related Phenom.* **82,** 125 (1996).
32. C. B. Stagarescu, L.-C. Duda, J. Downes, and K. E. Smith, unpublished, (1998).
33. N. Nücker, J. Fink, D. Schweitzer, and H. J. Keller, *Physica* **143B,** 482 (1986).